tureless and homogeneous while polyelectrolyte I yields coatings that appear segregated into two types of domains. Of even greater importance to the present study was the observation that polyelectrolyte I appears to retain its domain-forming tendency when mixed with auxiliary polyelectrolytes. The resulting coatings assume structures in which polyelectrolyte I apparently serves as a template that controls the morphology adopted by the composite coating. Coatings with structures similar to that in Figure 4C developed when polyelectrolyte I was mixed with several other auxiliary polyelectrolytes, indicating that the spontaneous tendency of I to form segregated domains dictates the morphologies adopted by the mixtures. However, the second polyelectrolyte in the mixtures is not an inert component. Its presence is essential to produce highly swollen coatings that exhibit hydrophilic domains with ion-exchange capacities much greater than those of polyelectrolyte I alone. The sizes of the hydrophilic domains obtained with the composite coatings are approximately two orders of magnitude larger than those that have been reported for the rather dissimilar and relatively permselective polyelectrolyte Nafion.[19] The much more highly swollen nature of the composite coatings we have prepared and their larger hydrophilic domains may result in rather low permselectivity.

Mixing polyelectrolyte I with the auxiliary polyelectrolytes also yields coatings that are much longer lived than those obtained from the auxiliary polyelectrolytes alone The greater coating stability probably results from some form of association of the polymeric chains of the two components in the mixtures coupled with a strong hydrophobic interaction between the electrode surface and the styrene groups of polyelectrolyte I. Whatever the molecular basis of the greater stability of the composite coatings, the data collected in Tables I and II show clearly that a property other than chemical composition must be important in determining the ion-exchange capacities and diffusional rates of counterions incorporated by the composite coatings. However, a two-domain structure alone is not adequate to ensure these attractive properties: Coatings prepared from polyelectrolyte I alone exhibit a two-domain structure (Figure 4B) but have much lower ion-exchange capacities and retain incorporated reactants rather poorly when transferred to pure supporting electrolyte solutions (Table I). Thus, the presence of segregated domains within polyelectrolyte coatings appears to be a necessary but not sufficient condition for obtaining the desirable properties we have described.

The idea that certain types of polyelectrolyte coatings on electrodes are made up of two (or more) domains has been suggested in previous studies,[6c,g] and considerable evidence supporting a segregated domain structure for Nafion membranes is available.[19] However, the notion that useful domain structures can be induced in polyelectrolyte coatings by using a strong domain-forming polymer as a template that controls the structure of coatings obtained from mixtures containing other components that have desirable properties is new. The examples offered in this study demonstrate the concept, but the full range of its applicability remains to be explored. The potential of composite coatings in which templating polymers define the overall morphology and auxiliary polyelectrolytes establish the electrostatic and chemical environment experienced by incorporated reactants seems broad and appealing. The flexibility such a strategy introduces for tailoring the properties of coatings to meet specific requirements should prove valuable both in practical applications and in fundamental investigations of the behavior of polyelectrolyte-coated electrodes.

Acknowledgment. This work was supported in part by the National Science Foundation and the U.S. Army Research Office. D.D.M. was the holder of a Graduate Fellowship sponsored by the Exxon Education Foundation. The assistance of Prof. J. P. Revel and Pat Koen in obtaining the electron micrographs was very helpful. We gratefully acknowledge the important contributions of Prof. Eishun Tsuchida and Dr. Kiyotaka Shigehara at Waseda University, Tokyo, to the synthesis of the polyelectrolytes in Figure 1.

Registry No. PVI, 26983-77-7; NDI, 96164-78-2; PEI, 26336-38-9; PLL, 25104-18-1; PVP, 25232-41-1; $Fe(CN)_6^{4-}$, 13408-63-4; $IrCl_6^{3-}$, 14648-50-1; Hg, 7439-97-6; C, 7440-44-0; ferrocene, 102-54-5.

Quenching and Possible Coulombic Complexation of the Pyrene–*N*,*N*-Dimethylaniline Exciplex by Tetraalkylammonium Salts

Rolfe J. Hartley and Larry R. Faulkner*

Contribution from the Department of Chemistry, University of Illinois, Urbana, Illinois 61801.
Received June 25, 1984

Abstract: Tetraalkylammonium salts are shown to quench the fluorescence of the pyrene–*N*,*N*-dimethylaniline exciplex in solvents of low dielectric constant. Linear Stern–Volmer plots are obtained for quenching of both lifetime and intensity in dioxane. However, mechanistic complications are implied by intercepts exceeding unity and by the unequal slopes of these plots. Qualitatively similar behavior is observed when the solvents and electrolytes are varied. Historic conductivity data indicate that the quenching species Q in dioxane are aggregates of electrolyte ions, probably ion pairs or quadrupoles. A proposed kinetic model is both qualitatively consistent with the experimental observations and quantitatively self-consistent. An emitting complex formed at a diffusion-controlled rate by an encounter between Q and an exciplex is postulated. The emitting complex is apparently quenched by subsequent encounters with additional Q at rates considerably below the encounter-limited value.

Since the discovery of polar exciplexes by Leonhardt and Weller,[1] there has been particular interest in these aggregates of unlike molecules that exhibit stable binding in excited electronic states but repulsive interactions in the ground state.[2-7] Many feature strong charge-transfer character and are bound essentially by Coulombic forces between the positive and negative moieties. Ample evidence has accumulated to indicate their general im-

(1) Leonhardt, v. H.; Weller, A. *Ber. Bunsenges. Phys. Chem.* **1963**, *67*, 791.

(2) Birks, J. B. "Photophysics of Aromatic Molecules"; Wiley: New York, 1970.

0002-7863/85/1507-3436$01.50/0 © 1985 American Chemical Society

portance as intermediates in photochemistry.[4-8] They may be particularly important in light-driven electron-transfer reactions, which are of general interest as a basis for photochemical energy conversion.[9-16]

They can be generated in several ways, but a common route is

$$^1A^* + D \rightarrow {}^1(A^-D^+)^* \quad (1)$$

where $^1A^*$ is an excited singlet molecule (such as pyrene) that acts as an electron acceptor, D is a donor (such as *N,N*-dimethylaniline), and $^1(A^-D^+)^*$ represents the singlet exciplex. This species is often sufficiently long lived to provide luminescence.[1-7]

$$^1(A^-D^+)^* \rightarrow A + D + h\nu \quad (2)$$

In photochemical energy conversion, one wishes to prevent the recombination of the paired charge carriers A^- and D^+, which can occur by internal relaxation of the exciplex. Instead, one would prefer to maneuver the system along a pathway leading to permanent separation of the carriers. Luminescence offers a useful means for observing such a process.

The quantum yield for exciplex fluorescence decreases and the yield of radical ions rises as the dielectric constant of the solvent increases, apparently because the radical ions are stabilized by dipolar solvation.[1-7] In solvents of high dielectric constant, the fluorescence is quenched completely, and only radical ions are obtained. Externally applied electric fields have also been observed to quench exciplex emission in poly-*N*-vinylcarbazole films doped with electron acceptors.[17-20] Given the known influence of electric fields on decay channels of exciplexes, it seems likely that simple bimolecular encounters between exciplexes and ions or aggregates of ions would also affect the fates of the exciplexes in useful ways. Electrolytes have been shown to affect the photoredox kinetics and cage escape yields in the photoredox quenching of electronically excited $Ru(bpy)_3^{2+}$;[21-24] however, the results were understood essentially in terms of the primary kinetic salt effect, an environmental concept. Our goal was to search for bimolecular elementary reactions between exciplexes and charged species or simple electrical multipoles.

We demonstrate here the quenching of exciplex fluorescence by electrolytes in solvents of low polarity. During the course of our work several related studies were reported. Simon and Peters[25-27] used picosecond absorption spectroscopy to examine the kinetics of reactions between ion pairs of various salts and photogenerated ion pairs of benzophenone radical anions ($BP^{\cdot-}$) and dialkylaniline radical cations ($DAA^{\cdot+}$). In media of low polarity, the contact ion pairs ($BP^{\cdot-}DAA^{\cdot+}$) are probably identical with the known[21] BP–DAA exciplexes. The reaction of interest to Simon and Peters[26,27] was an exchange, in which the cation from the attacking pair replaced $DAA^{\cdot+}$ as the partner to the benzophenone anion radical. To the extent that the $BP^{\cdot-}$ $DAA^{\cdot+}$ species can be identified as an exciplex, this process would be a quenching reaction. Of more direct relation to our results are the very recent papers by Kitamura et al.[28] and by McCullough and Yeroushalmi,[29] who reported essentially the quenching effect discussed here, although they did not examine the process in detail.

The dynamics are not simple. We suggest that the primary pyrene–*N,N*-dimethylaniline exciplex forms stoichiometric, emissive complexes with ion pairs or higher aggregates of the salts. These complexes are secondary species that can be regarded as chemical derivatives of the primary exciplex. Independent, complementary work has been carried out by Goodson and Schuster,[30] and their report is being submitted in parallel with this one. They corroborate the kinetic peculiarities and suggest an origin rooted in variable electrolyte association to orders exceeding simple pairing.

Experimental Section

Tetra-*n*-butylammonium fluoborate ($TBABF_4$), tetraethylammonium fluoborate ($TEABF_4$), tetra-*n*-butylammonium perchlorate (TBAP), and tetra-*n*-butylammonium hexafluorophosphate ($TBAPF_6$) were purchased from Southwestern Analytical Chemicals (Electrometric Grade). $TEABF_4$ was recrystallized three times from a mixture of methanol–petroleum ether, and the tetrabutylammonium salts were thrice recrystallized from an ethyl acetate–pentane mixture. Anthracene (99.99+%) and pyrene (99+%) were purchased from Aldrich and were used without further purification. *N,N*-Dimethylaniline (DMA) was obtained from Aldrich and was distilled under vacuum from calcium hydride just before use. The 1,4-dioxane and dichloromethane (Matheson Coleman and Bell, scintillation quality) were used as purchased. Pyridine (Aldrich Gold Label) was used without further purification. Cyclohexane was obtained from Burdick and Jackson (Distilled in Glass) and used as received.

Fluorescence lifetimes were measured with an EG&G ORTEC Model 9200 time-correlated single photon counting instrument.[31-33] An Apple II Plus microcomptuer carried out the functions of a multichannel analyzer through a custom-built interface to the ORTEC 9200. Calculations and data reduction were also carried out by the microcomputer. Samples were excited by an air-gap flashlamp manufactured by EG&G ORTEC. It typically had a pulse width at half intensity of 1.5–2.0 ns. A colored glass filter passing light from 330 to 360 nm was used to filter the excitation flash. The resulting fluoresence was observed through an Oriel type 5435 interference filter centered on 520 nm and having a 9-nm band-pass.

Fluorescence intensity measurements were made with an Aminco-Bowman fluorescence spectrometer. Excitation was carried out at 90° geometry with the 334-nm Hg line from a 200 W Xe–He lamp. Emission was detected with a Hamamatsu R928 photomultiplier tube, and the photocurrent was monitored with a Keithley Model 610B electrometer.

All measurements in dichloromethane were made on sealed samples that had been deaerated by at least 5 freeze–pump–thaw cycles on a vacuum line. Samples in dioxane and pyridine were prepared at first by that technique. Later, is was found to be as satisfactory to deaerate the solutions by bubbling them with solvent-saturated nitrogen. With use of a specially constructed bubbler cell, lifetimes were obtained while the

(3) Weller, A. *Pure Appl. Chem.* **1968**, *16*, 115.
(4) Gordon, M.; Ware, W. R.; De Mayo, P.; Arnold, D. R., Eds. "The Exciplex"; Academic Press: New York, 1975.
(5) Froehlich, P.; Wehry, E. L. In "Modern Fluorescence Spectroscopy"; Wehry, E. L., Ed.; Plenum: New York, 1976; Vol. 2, p 319–438.
(6) Masuhara, H.; Mataga, N. *Acc. Chem. Res.* **1981**, *14*, 312.
(7) Davidson, R. S. *Adv. Phys. Org. Chem.* **1983**, *19*, 43.
(8) Mattes, S. L.; Farid, S. *Chem. Res.* **1982**, *15*, 80.
(9) Archer, M. D. *J. Appl. Electrochem.* **1975**, *5*, 117.
(10) Porter, G.; Archer, M. D. *Interdisc. Sci. Rev.* **1976**, *1*, 119.
(11) Whitten, D. G. *Acc. Chem. Res.* **1980**, *13*, 82.
(12) Wrighton, M. S., Ed. *ACS Adv. Chem. Ser.* **1980**, 184.
(13) Grätzel, M. *Ber. Bunsenges. Phys. Chem.* **1980**, *84*, 981.
(14) Grätzel, M. *Acc. Chem. Res.* **1981**, *14*, 376.
(15) Faulkner, L. R.; Suib, S.L.; Renschler, C. L.; Green, J. M.; Bross, P. R. In "Chemistry in Energy Production", Wymer, R. K., Keller, O. L., Eds.; American Chemical Society: Washington, 1982; ACS Symp. Ser., pp 99–113.
(16) Zamarev, K. I.; Parmon, V. N. *Usp. Khim.* **1983**, *52*, 1433; *Russ. Chem. Rev.* **1983**, *52*, 817.
(17) Yokoyama, M.; Endo, Y.; Mikawa, H. *Chem. Phys. Lett.* **1975**, *34*, 597.
(18) Yokoyama, M.; Endo, Y.; Mikawa, H. *Bull. Chem. Soc. Jpn.* **1976**, *49*, 1538.
(19) Yokoyama, M.; Endo, Y.; Matsubara, A.; Mikawa, H. *J. Chem. Phys.* **1981**, *75*, 3006.
(20) Yokoyama, M.; Shimokihara, S.; Matsubara, A.; Mikawa, H. *J. Chem. Phys.* **1982**, *76*, 724.
(21) Meisel, D.; Matheson, M. *J. Am. Chem. Soc.* **1977**, *99*, 6577.
(22) Meisel, D.; Rabani, J.; Meyerstein, D.; Matheson, M. *J. Phys. Chem.* **1978**, *82*, 985.
(23) Jonah, C. D.; Matheson, M. S.; Meisel, D. *J. Phys. Chem.* **1979**, *83*, 257.
(24) Kalyanasundaram, K.; Neumann-Spallart, M. *Chem. Phys. Lett.* **1982**, *88*, 7.
(25) Simon, J. D.; Peters, K. S. *J. Am. Chem. Soc.* **1981**, *103*, 6403.
(26) Simon, J. D.; Peters, K. S. *J. Am. Chem. Soc.* **1982**, *104*, 6142.
(27) Simon, J. D.; Peters, K. S. *J. Am. Chem. Soc.* **1983**, *105*, 4875.
(28) Kitamura, N.; Imabayashi, S.; Tazuke, S. *Chem. Lett.* **1983**, 455.
(29) McCullough, J. J.; Yeroushalmi, S. *J. Chem. Soc., Chem. Commun.* **1983**, 254.
(30) Goodson, B. E.; Schuster, G. B., submitted.
(31) Ware, W. R. In "Creation and Detection of the Excited State"; Lamola, A. A., Ed.; Marcel Dekker: New York, 1971; Vol. 1A.
(32) Renschler, C. L.; Faulkner, L. R. *Faraday Discuss. Chem. Soc.* **1980**, *70*, 311.
(33) Brazas, J. C. Ph.D. Thesis, University of Illinois at Urbana–Champaign, 1983.

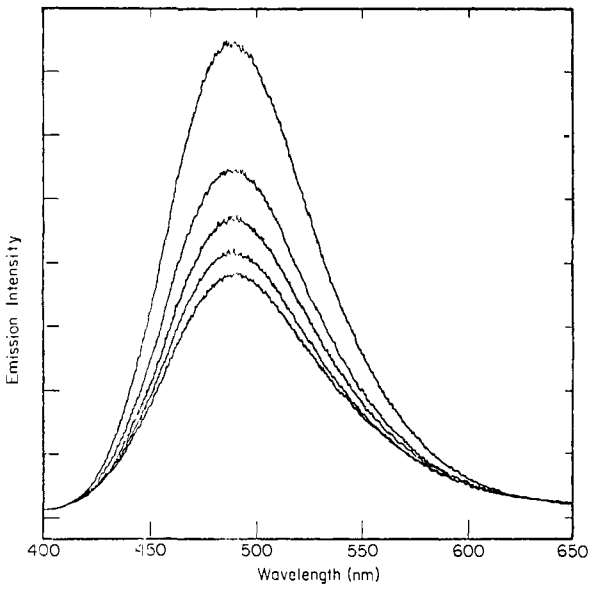

Figure 1. Uncorrected emission spectra of the pyrene–DMA exciplex in dioxane. Top curve is for no $TBAF_4$ added. Successively lower curves are for 1, 2, 3, and 4 mM $TBABF_4$ added, respectively.

sample was continuously purged with nitrogen. Intensity measurements were made after bubbling nitrogen through the sample solution in a standard quartz cuvette. During the actual measurements, the bubbling was stopped, but an oxygen-free blanket of nitrogen was allowed to remain over the solution.

The temperature for lifetime experiments was 24 ± 1 °C, while the temperature for most intensity measurements was 30 ± 2 °C. Later in this study, a thermostated cell holder was employed, and all of the carefully analyzed data discussed below for dioxane solutions were obtained with this device at 23.5 °C.

Quantum yields were obtained via the conventional method for optically dilute solutions involving comparison with a standard emitter.[34,35] Anthracene in cyclohexane was used as the reference compound and was assumed to have a quantum yield of 0.30.[2] The emission monochromator and detector were calibrated both with a tungsten lamp,[34] standardized to a color temperature of 2860 K by the Electrical Testing Laboratories (New York, NY), and with the quantum counter technique of Melhuish.[34,36] The correction functions were isomorphic in the region of overlap. Emission spectra were digitized by using a Summagraphics digitizing tablet operated as a peripheral device to a Nova 820 minicomputer. Storage and correction of the spectra was carried out with the Nova 820 system.

Results and Discussion

In all of the work described here, DMA concentrations near 100 mM were used to ensure quantitative conversions of pyrene-excited (pyrene = Py) singlets into the exciplex $^1(Py^-DMA^+)^*$ within a few nanoseconds after excitation. The contribution of pyrene fluorescence to the emission spectrum is therefore very small, as Figure 1 attests. In electrolyte-free solutions, the luminescence decay after an initial transient (<10 ns) was a pure exponential reflecting first-order relaxation of the exciplex without contributions from pyrene fluorescence or from the dynamics of exciplex formation. At 94 mM DMA and 1×10^{-5} M pyrene in dioxane at 23.5 °C, the lifetime was $\tau_0' = 119.3 \pm 0.6$ ns. Under the same conditions, the fluorescence quantum yield of the exciplex was measured to be $\phi_f' = 0.53$. There was only a very small dependence of the lifetime on DMA concentration at room temperature and none at all at higher temperatures, hence the formation of triple exciplexes[5,7] seems unimportant. In the analysis below, we consider the immediate result of light absorption to be the production of $^1(Py^-DMA^+)^*$.

The fluorescence intensity of the pyrene–DMA exciplex was clearly quenched by tetraalkylammonium salts, as Figure 1 illustrates. Table I shows that there was no change in the peak position of the emission band with increasing salt concentration, although a broadening of the emission band is evident in the long-wavelength side of the spectrum. Knibbe et al. have observed that both the lifetime and fluorescence intensity of the anthracene–diethylaniline exciplex decrease with increasing dielectric constant,[37] and other studies have shown that the emission maximum of the pyrene–DMA exciplex shifts to the red as the solvent becomes more polar.[2-7,38,39] While the broadening of the emission band in Figure 1 indicates that the electronic structure of the exciplex is changed by interaction with the electrolyte, the lack of a red shift for the peak position suggests that the observed

Table I. Emission Band Shape for the Pyrene–DMA Exciplex[a]

	wavelength/nm at I/I_{max} = [b]				
$[TBABF_4]$/mM	0.20 (blue)	0.50 (blue)	1.00	0.50 (red)	0.20 (red)
0	440	458	499	548	584
1.00	438	457	498	548	588
2.00	439	458	496	551	592
3.00	438	457	499	552	594
4.00	437	457	494	554	596

[a] Corrected spectra for curves in Figure 1. [b] Wavelength positions at which equivalent fractions of peak intensity are reached. (blue) = high energy side of peak; (red) = low energy side. Precision is ±1 nm for all values except peak, which is ±3 nm.

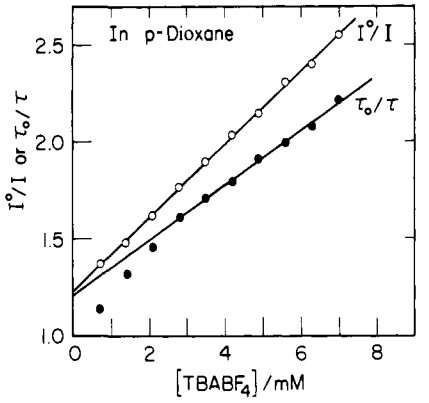

Figure 2. Stern–Volmer plots for the quenching of the pyrene–DMA exciplex in dioxane. [Py] = 1×10^{-5} M, [DMA] = 94 mM, τ_0' = 119.3 ns, T = 23.5 °C. Intensities are measured at peak maximum.

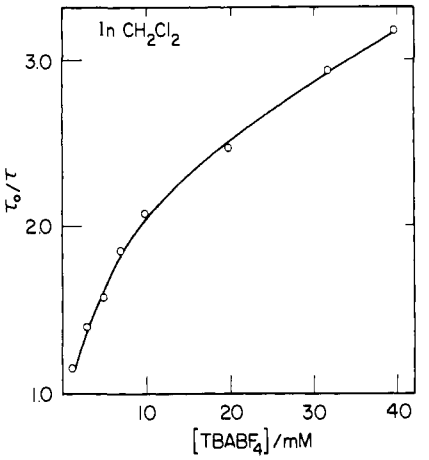

Figure 3. Stern–Volmer plot for lifetime quenching of the pyrene–DMA exciplex by $TBABF_4$ in dichloromethane. [DMA] = 97 mM, [Py] = 1×10^{-5} M, τ_0' = 73.8 ns.

(34) Parker, C. A. "Photoluminescence of Solutions"; Elsevier: Amsterdam, 1968.
(35) Demas, J. N.; Crosby, G. A. *J. Phys. Chem.* **1971**, *75*, 991.
(36) Melhuish, W. H. *J. Opt. Soc. Am.* **1962**, *52*, 335.
(37) Knibbe, H.; Röllig, K.; Schäfer, F. P.; Weller, A. *J. Chem. Phys.* **1967**, *47*, 1184.
(38) Beens, H.; Knibbe, H.; Weller, A. *J. Chem. Phys.* **1967**, *47*, 1183.
(39) Beens, H.; Weller, A. In "Organic Molecular Photophysics"; Birks, J. B., Ed.; Wiley: New York, 1975; Vol. 2, p 159.

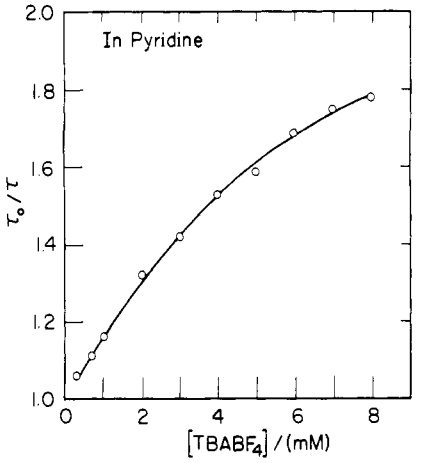

Figure 4. Stern–Volmer plot for lifetime quenching of the pyrene–DMA exciplex by $TBABF_4$ in pyridine. [DMA] = 97 mM, [Py] = 1×10^{-5} M, $\tau_0' = 31.7$ ns.

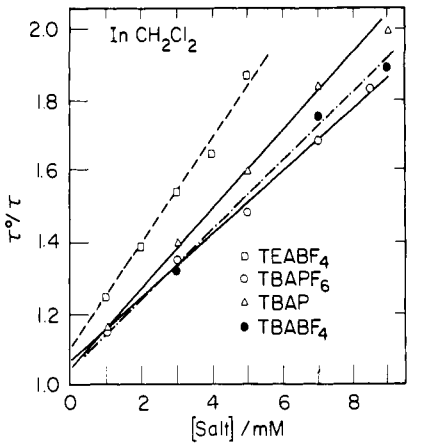

Figure 5. Stern–Volmer plots for lifetime quenching of the pyrene–DMA exciplex in dichloromethane by various salts. [DMA] = 97 mM, [Py] = 1×10^{-5} M, $\tau_0' = 73.8$ ns.

quenching does not result simply from a change in the average bulk dielectric environment experienced by the exciplex, but it is more likely a kinetic process.

Lifetime Measurements. Figure 2 contains a Stern–Volmer plot for quenching of the exciplex lifetime by $TBABF_4$ in dioxane. The plot becomes linear only at higher salt concentrations. This feature alone is an indication that the quenching mechanism does not involve a single elementary step.

Qualitatively similar behavior exists for other solvents and electrolytes, as one can see in Figures 3, 4, and 5. Figures 3 and 4 show that the Stern–Volmer plots for solutions in dichloromethane and pyridine are not linear, whereas Figure 5 demonstrates that the identity of the electrolyte is qualitatively unimportant.

Concentrations of $TBABF_4$ between 1 and 24 mM in dioxane had no effect on the pyrene excimer lifetime, which remained at 63.5 ns for pyrene concentrations of 10 mM. Since the pyrene excimer is believed to be apolar and bound by excitation resonance, this result supports the idea that electrolyte quenches the pyrene–DMA exciplex by electrostatic disruption of its Coulombic binding forces.

Intensity Quenching. Figure 2 offers a comparison of Stern–Volmer plots for quenching of the emission intensity and the lifetime of the pyrene–DMA exciplex in dioxane by $TBABF_4$. Both plots are linear at salt concentrations above 2 mM, and the linear segments have intercepts greater than unity. However, the slope for intensity quenching is about 30% larger than the slope for lifetime quenching. Part of this difference comes from broadening induced by the electrolyte, but a plot of intensity quenching on a quantum-yield basis, made by integrating the corrected spectra, still shows a markedly larger slope than is found for lifetime quenching. The high intercepts in intensity-quenching plots are actually apparent in the data reported by Kitamura et al.,[28] but no attention was called to them. A successful model for the quenching process must explain this peculiar behavior.

Table II. Estimated Free Ion Concentrations

solvent	ϵ^b	relative free ion concentrations[a]		
		K^c	at C = 1 mM	at C = 5 mM
pyridine	13.24_{20}	5.37×10^2	72%	45%
CH_2Cl_2	8.93_{25}	1.41×10^4	23%	11%
p-dioxane	2.23_{25}	1.76×10^{17}	0%	0%

[a] $[TBA^+]$ or $[BF_4^-]/C$, as a percentage of C, where C is the analytical concentration of $TBABF_4$. [b] Mann, C. K. *Electroanal. Chem.* **1969**, *3*, 57. [c] From the Fuoss equation.

Identity of Quenching Species. Ionic compounds may exist in solution as free ions, ion pairs, triple ions, or higher aggregates. The species present in any particular solution depends on dielectric constant, ionic strength, ionic size, and specific ion–solvent interactions.[40-45]

Solvent-separated ion pairs occur when the comparatively strong electric fields of small ions cause the formation of a coordination sphere of solvent molecules around each ion. Bulky ions with comparatively weak electric fields do not interact strongly enough with the dipoles of the solvent to acquire a coordination sphere of solvent molecules. Thus, bulky ions form contact pairs in aprotic solvents in low dielectric constant. It is highly probable that $TBABF_4$ forms contact ion pairs, rather than solvent-separated ion pairs.

Under that assumption, one can calculate the equilibrium constant for the ion association,

$$TBA^+ + BF_4^- \rightarrow TBA^+BF_4^- \quad (3)$$

using the theoretical equation derived by Fuoss[42]

$$K = \frac{4\pi N a^3}{3000} \exp\frac{e_0^2}{a\epsilon k_B T} \quad (4)$$

Here, N is Avogadro's number, a is the center-to-center distance in the contact ion pair, e_0 is the electronic charge, ϵ is the dielectric constant, k_B is Boltzmann's constant, and T is the absolute temperature. Taking a as the sum of the ionic radii [$r(+) = 4.09$ Å[46] and $r(-) = 2.16$ Å[47]], we obtain the results summarized in Table II. The concentration of free ions is expected to vary enormously in the solvents studied. Since the degree of quenching does not vary correspondingly at, for example, a salt concentration of 5 mM in the different solvents, it is unlikely that free ions are the sole quenching agents. In dioxane, they probably play no role at all.

In the more polar media, free ions may be important, and their variable degrees of participation over the examined concentration ranges may account for the nonlinearities in Stern–Volmer plots observed with pyridine and methylene chloride solutions. In the following discussion, we stress observations with dioxane solutions, because the linearity of the quenching plots suggests the simplicity of a single effective quencher.

The identity of that species is difficult to be sure about, because the conductivities of electrolytes in pure dioxane have not been examined. Even so, triple ions can be ruled out. Equilibrium constants presented by Fuoss and Kraus[48] for tetraisoamyl-

(40) Kraus, C. A. *J. Phys. Chem.* **1954**, *58*, 673.
(41) Kraus, C. A. *J. Phys. Chem.* **1956**, *60*, 129.
(42) Fuoss, R. M. *J. Am. Chem. Soc.* **1958**, *80*, 5059.
(43) Szwarc, M. *Acc. Chem. Res.* **1969**, *2*, 87.
(44) Szwarc, M., Ed. "Ions and Ion Pairs in Organic Reactions"; Wiley: New York, 1972; Vol. 1 and 2.
(45) Meyer, U. *Pure Appl. Chem.* **1975**, *41*, 291.
(46) De Ligny, C. L.; Denessen, H. J. M.; Alfenaar, M. *Recl. Trav. Chim. Pays-Bas* **1971**, *90*, 1265.
(47) Halliwell, H. F.; Nyburg, S. C. *Trans. Faraday Soc.* **1963**, *59*, 1126.

Table III. Measured Quantities for Exciplex Quenching in Dioxane[a]

quantity	source	value	uncertainty[b]
ϕ_f'	measured	0.53	[c]
τ_0', ns	measured	119.3	±0.6
$(k_f' + k_i')$, s^{-1}	$1/\tau_0'$	8.38×10^6	$\pm 0.04 \times 10^6$
ϕ_f'/ϕ_f''	intensity intercept	1.23	±0.02
$\phi_f' k_q/k_f''$, M^{-1}	intensity slope	155	±4
τ_0'/τ_0''	lifetime intercept	1.29	±0.02
$k_q/(k_f' + k_i')$, M^{-1}	lifetime slope	139	±4

[a] All data taken at 23.5 °C. [b] Standard deviations. [c] One measurement.

ammonium nitrate in 99.40% dioxane–0.60% water indicate that the concentrations of these species would only be about 10^{-8}–10^{-7} M in our systems. The most likely remaining candidates are ion pairs and quadrupoles. The association of ion pairs into quadrupoles and higher aggregates is known to range from negligible to extensive degrees for various salts in benzene over the concentration range of interest here.[40,41] The extent of association is a function of ion size and dipole moment. In our systems, this process would be relatively discouraged by the slightly greater polarity of dioxane and the presence of 1% DMA in the medium. We acknowledge that the active quencher in our experiments with dioxane could be a quadrupole (or even a higher aggregate), but we develop the model as though it were an ion pair.

Mechanistic Concepts. Further discussion is based on the primary measurements in Table III. The slopes and intercepts of the plots tabulated there for intensity quenching were obtained on a quantum yield basis. The stated precisions of all Stern–Volmer parameters are standard deviations of the mean values obtained from six independent data sets. A crucial point in the interpretation is the likelihood that the quenching of intensity is not isomorphic with the quenching of lifetime. For the linear parts of the plots (comprising all concentrations for intensity quenching and those greater than 2 mM for lifetime quenching), our results indicate that a statistically significant difference exists in the slopes at a confidence level exceeding 95%. Besides, the lack of isomorphic quenching at low electrolyte concentrations is obvious from inspection.

This kind of behavior is in many ways typical of classical "static" quenching.[2,34] The high intercept for intensity quenching in that case is attributed to the formation of a nonluminescent complex between the ground-state fluorophore and the quenching species. The kinetics describing this behavior reflect essentially instantaneous quenching of the excited state by an associated species, as well as diffusional quenching of unassociaed fluorophores by a mobile quencher. The exciplex studied here is first formed by a diffusional encounter between DMA and $^1Py^*$; thus the idea of a preexisting complex between the quencher and the ground-state precursor to the excited state is not reasonable, although the results could be explained in a static model if there were prior association between $TBA^+BF_4^-$ and either pyrene or DMA.

A ground-state interaction between pyrene and a polar species can be detected by changes in the fluorescence emission spectrum of pyrene. The intensity of the symmetry-forbidden 0–0 vibronic emission band of pyrene increases with the increasing dipole moments of associated solvent molecules, while the stronly allowed 0–3 vibronic transition remains unaffected.[49] Thus, the ratio of the 0–3 and the 0–0 emission intensities is a useful diagnostic, and it has been used by Kalyanasundaram and Thomas as a probe of polarity in micellar systems.[50] We measured the ratio for solutions in dioxane-containing 0–25 mM $TBABF_4$, and it remained constant within 2% over the entire range. Pyrene apparently does not associate with the electrolyte in the ground state.

Absorption spectra for DMA solutions containing $TBABF_4$ at 0–25 mM also showed no changes as the $TBABF_4$ concentration was elevated; hence, interaction in the ground state between DMA and $TBABF_4$ is not evident either. Besides, such an interaction can be ruled out as a basis for the observed quenching simply by considering relative concentrations. In most of our experiments, the concentration of DMA was 94 mM. At 1 mM $TBABF_4$, the quenching effect was about 30%. On statistical grounds alone, this degree of quenching cannot be understood static association of the salt with DMA. These observations, together with nonisomorphic intensity and lifetime quenching, indicate that the peculiarities of the quenching plots reflect excited-state dynamics, rather than ground-state dynamics.

Scheme I

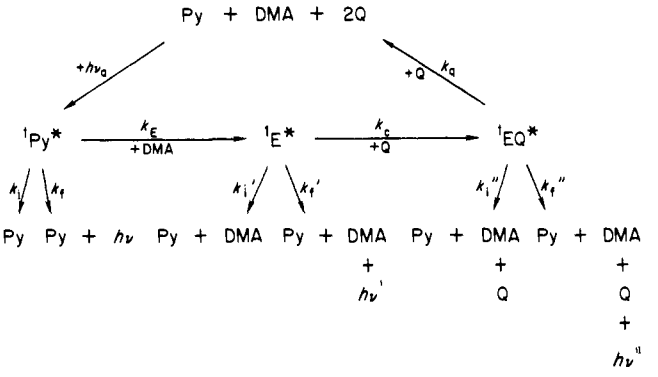

Quenching behavior similar to that observed here would apply if the exciplex formed a complex with the quencher on a short times scale compared with that of observation, and the band broadening induced by the salt suggests that there is an interaction between the exciplex and the quencher lasting over the lifetime of the emission. We have considered several particular mechanisms, but only one has produced quantitative and qualitative agreement with the data. It is developed in the next section. The others will be summarized briefly later.

Kinetic Model. The workable mechanism is illustrated in Scheme I. There, $^1Py^*$ and DMA are excited singlet pyrene and *N*,*N*-dimethylaniline, respectively; $^1E^*$ is the normal exciplex $^1(Py^-DMA^+)^*$; Q is the quenching species (presumed in ion pair); and $^1EQ^*$ is a second emitting complex formed by the interaction of the Q with the exciplex, perhaps $^1(Py^-DMA^+{:}TBA^+ClO_4^-)^*$. The k_f's and k_i's are rate constants for the radiative and nonradiative deactivation of the corresponding excited-state species, respectively. Rate constants for exciplex formation, emitting complex formation, and emitting complex quenching are represented by k_E, k_c,and k_q, respectively.

Analysis of Scheme I reveals that the expected Stern–Volmer slopes and intercepts are dependent upon the method used to create the excited state. In the following discussion, I_a is the rate of light absorption by pyrene, I_f^0 is the fluorescence intensity in the absence of quencher, and I_f is the fluorescence intensity with quencher present. All have dimensions of einsteins per unit volume. The unquenched lifetimes of the exciplex $^1E^*$ and the emitting complex $^1EQ^*$ are given by $\tau_0' = (k_f' + k_i')^{-1}$ and $\tau_0'' = (k_f'' + k_i'')^{-1}$, respectively. The unquenched quantum yields of the exciplex and the emitting complex are $\phi_f' = k_f'/(k_f' + k_i')$ and $\phi_f'' = k_f''/(k_f'' + k_i'')$.

In the treatment of steady illumination, we first assume that the concentration of DMA is sufficiently high to assure that each $^1Py^*$ is converted rapidly to an exciplex $^1E^*$. Then,

$$[^1E^*] = I_a\tau' \tag{5}$$

$$[^1EQ^*] = k_c[Q][^1E^*]\tau'' \tag{6}$$

The fluorescence intensity is generally

$$I_f = (k_f' + k_f''k_c[Q]\tau'')[^1E^*] \tag{7}$$

but at zero electrolyte concentration it is simply

$$I_f^0 = k_f'I_a/(k_f' + k_i') \tag{8}$$

Division of eq 8 by eq 7 yields an analogue to the Stern–Volmer relationship for intensity quenching:

(48) Fuoss, R. M.; Kraus, C. A. *J. Am. Chem. Soc.* **1933**, *55*, 2387.
(49) Nakajima, A. *J. Lumin.* **1976**, *11*, 429.
(50) Kalyanasundaram, K.; Thomas, J. K. *J. Am. Chem. Soc.* **1977**, *99*, 2039.

$$\frac{I_f^0}{I_f} = \frac{\dfrac{k_f'}{k_f' + k_i'}}{\dfrac{k_f'}{k_f' + k_i' + k_c[Q]} + \dfrac{k_f'' k_c[Q]}{(k_f'' + k_i'' + k_q[Q])(k_f' + k_i' + k_c[Q])}} \quad (9)$$

An important simplification can be made for most of the studied range of [Q], if one assumes that [^{1}EQ*] is formed by a diffusion-controlled reaction between a quencher and an exciplex. Then for $k_c \cong 2 \times 10^{10}$ M^{-1} s^{-1} and [Q] > 2 mM, the product k_c[Q] becomes greater than about 4×10^7 s^{-1}. Since $(k_f' + k_i') = 1/\tau_0' = 8.38 \times 10^6$ s^{-1}, then over most of the studied concentration range $k_c[Q] \gg (k_f' + k_i')$. The intensity quenching relationship simplifies to

$$\frac{I_f^0}{I_f} = \frac{\phi_f'}{\phi_f''} + \frac{\phi_f' k_q}{k_f''}[Q] \quad (10)$$

Thus, a linear plot is expected in the Stern–Volmer format, although the intercept, as the ratio of quantum yields, generally would differ from unity. In the application of this equation, total intensities, integrated over the emission spectrum, must be used.

A similar, but different, Stern–Volmer form comes from a consideration of the quenching of lifetime. In a solution with DMA, the lifetime of pyrene is

$$\tau_{Py} = (k_f + k_i + k_E[DMA])^{-1} \quad (11)$$

At high concentrations of DMA, the product k_E[DMA] dominates this expression. Since [DMA] $\cong$ 0.1 M and $k_E \cong 2 \times 10^{10}$ M^{-1} s^{-1}, the lifetime of the pyrene singlet is only about 500 ps. The formation of the exciplex therefore occurs almost instantaneously by comparison to the time domain over which the lifetime is measured. Assuming truly instantaneous formation of the exciplex, the decay of the initial exciplex population ($[^1E^*]_0$) is

$$[^1E^*] = [^1E^*]_0 \exp(-t/\tau_0' - k_c[Q]t) \quad (12)$$

From Scheme I, the time-dependent concentration of emitting complex can be found by writing

$$\frac{d[^1EQ^*]}{dt} = k_c[Q][^1E^*] - [^1EQ^*]/\tau'' \quad (13)$$

where $\tau'' = (k_f'' + k_i'' + k_q[Q])^{-1}$.

At quencher concentrations above 2 mM and with k_c regarded as about 2×10^{10} M^{-1} s^{-1}, the time $1/k_c[Q]$ is less than 25 ns. Since the lifetime is measured over a much larger time domain (400–800 ns), the second exponential term in eq 12 drives the population of ^{1}E* virtually to zero. Under these conditions, only ^{1}EQ* supplies significant emission, and the apparent "unquenched" lifetime of the emitting complex presented to the quencher becomes $\tau_0'' = (k_f'' + k_i'')^{-1}$. The observed lifetime is then τ'', and the Stern–Volmer equation for lifetime quenching is

$$\frac{\tau_0'}{\tau''} = \frac{\tau_0'}{\tau_0''} + k_q \tau_0'[Q] \quad (14)$$

Again, a linear plot is predicted. The intercept, which is the ratio of lifetimes, would generally differ both from unity and from the intercept of the intensity-quenching plot. The slopes of the lifetime-quenching and intensity-quenching plots would also differ. Thus, the observed behavir of the dioxane system shows qualitative agreement with the model under conditions that can reasonably be assumed to exist.

Table III shows the primary experimental measurements and their identification with the parameters of this scheme. Table IV lists the values of individual parameters that can be determined from the primary data. The value of k_q depends on the identification of Q as the ion pair. If it is the quadrupole instead, then k_q would be twice as large. Even so, for any reasonable state of aggregation in Q, k_q is probably less than diffusion controlled. Since the intercepts of the intensity-quenching and lifetime-quenching plots have similar values, it follows that $k_f' \cong k_f''$. That is, the difference in the quantum yields of the emitting complex and exciplex would be entirely due to more efficient nonradiative decay in ^{1}EQ*.

Table IV. Evaluated Parameters for Scheme I[a]

parameter	source	value	uncertainty[b]
k_E, M^{-1} s^{-1}	assumed	2×10^{10}	
k_c, M^{-1} s^{-1}	assumed	2×10^{10}	
τ_0', ns	measured	119.3	±0.6
ϕ_f'	measured	0.53	*c*
τ_0'', ns	lifetime intercept	93	±2
$k_f' + k_i'$, s^{-1}	$1/\tau_0'$	8.38×10^6	$\pm 0.04 \times 10^6$
$k_f'' + k_i''$, s^{-1}	$1/\tau_0''$	1.08×10^7	$\pm 0.02 \times 10^7$
k_q, M^{-1} s^{-1}	lifetime slope	1.16×10^9	$\pm 0.03 \times 10^9$
k_f', s^{-1}	ϕ_f'/τ_0'	4.4×10^6	*d*
k_i', s^{-1}	$k_f' + k_i'$	4.0×10^6	*d*
ϕ_f''	intensity intercept	0.43	*d*
k_f'', s^{-1}	ϕ_f''/τ_0''	4.6×10^6	*d*
k_i'', s^{-1}	$k_f'' + k_i''$	6.2×10^6	*d*

[a] At 23.5 °C. Evaluations are made from primary data in Table III. [b] Standard deviations. [c] Single measurement. Probably uncertainty ~10%. [d] All calculated using ϕ_f'. Probable uncertainty ~10–15%.

In Table IV, one can see that the intensity-quenching slope was not used to determine any individual parameter. Five measurements (τ_0', ϕ_f', intensity intercept, lifetime slope, lifetime intercept) provided all five kinetic parameters (k_i', k_f', k_i'', k_f'', and k_q). The intensity-quenching slope remains as a basis for checking the internal consistency of this model. The relations derived above indicate that the expression [lifetime slope × intensity intercept]/[intensity slope × lifetime intercept] should be unity. The calculated value is 0.86 ± 0.04. Even though the statistical uncertainty is sufficiently small that random errors probably would not give rise to the differences between this value and unity, one must allow an additional tolerance for systematic error in choosing the linear region of the lifetime plot. This choice particularly affects the lifetime intercept and could involve an error great enough to account for the difference between the calculated and observed intensity slopes. (Compare, for example, Figure 2 with the averages in Table III.) Thus the model proposed in Scheme I appears reasonably self-consistent in a quantitative sense.

Other Mechanisms. We have also considered a model in which ^{1}EQ* is nonfluorescent and is in equilibrium with ^{1}EQ*. The complex ^{1}EQ* is regarded as quenchable by species Q. This model predicts Stern–Volmer plots with intercepts of unity, hence it was discarded.

Finally we considered the case in which ^{1}EQ* exists in reversible kinetic balance with ^{1}E*, but without additional quenching of ^{1}EQ* by Q. This case does not produce linear Stern–Volmer plots, hence it was also discarded.

Goodson and Schuster, in their complementary paper to this one,[30] propose that the nonlinear Stern–Volmer plots for quenching of the pyrene–1,4-dicyanobenzene exciplex by electrolytes are caused by association of ion pairs into quadrupoles. They present osmometric data in support of such an association. This kind of effect would explain most of our observations, too, and relying on it entirely is an attractively simple approach to the problem. On the other hand, it is not consistent with the failure of the system to show isomorphic intensity and lifetime quenching. The fluorescence quantum yield is linked directly to the lifetime via the radiative rate constant. If all of the peculiarities in the Stern–Volmer plots arose entirely from ground-state equilibria, there would be no basis for expecting the constant of proportionality k_f' to change, and isomorphic behavior ought to exist.

We do believe that electrolyte aggregation is important in the chemistry of this kind of system, but on the basis of our results there appears to be a more elaborate story. At present, it is dangerous to attempt detailed comparisons between systems, because different association equilibria and quenching dynamics probably apply in the various systems that have been studied, particularly if different media are involved. Additional experi-

ments are needed to clarify the identities of the quenching species and to test for the general existence of nonisomorphic intensity and lifetime quenching.

Acknowledgment. We are grateful to G. B. Schuster and B. E. Goodson for sharing their results and ideas with us, and we are pleased to acknowledge support of this work by the National Science Foundation under Grants CHE-81-06026 and CHF 83-15177.

Registry No. $TBABF_4$, 429-42-5; $TEABF_4$, 429-06-1; TBAP, 1923-70-2; $TBAPF_6$, 3109-63-5; DMA, 121-69-7; pyrene, 129-00-0.

Electrocatalysis at Redox Polymer Electrodes with Separation of the Catalytic and Charge Propagation Roles. Reduction of O_2 to H_2O_2 as Catalyzed by Cobalt(II) Tetrakis(4-*N*-methylpyridyl)porphyrin

Fred C. Anson,*† Ching-Long Ni,† and Jean-Michel Saveant*‡

Contribution No. 7130 from the Division of Chemistry and Chemical Engineering, Arthur Amos Noyes Laboratories, California Institute of Technology, Pasadena, California 91125, and the Laboratoire d'Electrochimie, Universite de Paris VII, Tour 44-45, 75251 Paris, Cedex 05, France.
Received December 4, 1984

Abstract: The kinetics of the reduction of O_2 by $Ru(NH_3)_6^{2+}$ as catalyzed by cobalt(II) tetrakis(4-*N*-methylpyridyl)porphyrin are described both in homogeneous solution and when the reactants are confined to Nafion coatings on graphite electrodes. The catalytic mechanism is delineated and the factors that can control the total reduction currents at Nafion-coated electrodes are specified. A kinetic zone diagram for analyzing the behavior of catalyst–mediator–substrate systems at polymer-coated electrodes is presented and utilized in identifying the current-limiting processes. Good agreement is demonstrated between calculated and measured reduction currents at rotating disk electrodes. The experimental conditions that will yield the optimum performance of coated electrodes are discussed, and a relationship is derived for the optimal coating thickness.

Nafion coatings on electrodes offer unusually stable environments for attaching reactants to electrode surfaces.[1,2] The attributes of such coatings were exploited in a recent study of the catalysis of the electroreduction of dioxygen by cobalt tetraphenylporphyrin incorporated in Nafion coatings on graphite electrodes.[2d] It was necessary to incorporate a mediator redox couple such as $Ru(NH_3)_6^{3+/2+}$ into the Nafion coating along with the cobalt porphyrin catalyst in order to carry electrons from the electrode surface to the essentially immobile catalyst sites. The resulting three-component coating (Nafion, catalyst, redox mediator) provided an effective means for the electroreduction of dioxygen, albeit at a potential determined by the formal potential of the redox mediator.[2d] Three-component coatings allow the catalytic and charge propagation roles to be assigned to separate reactants that can be selected so as to maximize the overall rate of reaction of the substrate. It was therefore of interest to analyze the kinetics of dioxygen reduction by such a three-component electrode coating to understand how best to optimize experimental conditions in order to achieve high catalytic efficiency. This report is devoted to a kinetic analysis of a system in which cobalt(II) tetrakis(4-*N*-methylpyridyl)porphyrin was employed as the catalyst for the reduction of dioxygen to hydrogen peroxide with $Ru(NH_3)_6^{3+/2+}$ as the redox mediator. The water solubility of the catalyst allowed the kinetics to be measured in homogeneous solution as well as with the catalyst and mediator incorporated in Nafion coatings on rotating graphite disk electrodes. In both cases, the reaction appears to follow a "preactivation" mechanism in which only a preformed dioxygen-catalyst adduct is able to accept electrons from the redox mediator at a high rate. The reaction scheme thus involves a combination of "chemical catalysis" (formation of the adduct) and "redox catalysis" (outer-sphere reduction of the adduct) in the senses defined and analyzed by Andrieux et al.[3] Such preactivation mechanisms seem likely to be among the most frequently encountered in practical applications of electrodes coated with redox polymers. For example, the utilization of biological catalysts such as metalloenzymes as electrocatalysts[4] is likely to involve preactivation mechanisms and may often require separate redox mediators to provide rapid charge propagation throughout electrode coatings. For these reasons, we have analyzed the kinetic behavior of this first example of a preactivation catalytic mechanism at a redox polymer electrode in some detail and present our results in this report.

Experimental Section

Materials. $Ru(NH_3)_6Cl_3$ (Strem Chemical Co.) was purified according to the procedure of Pladziewicz et al.[5] Standard solutions of $Ru(NH_3)_6^{3+}$ were prepared by dissolving accurately weighed samples of $Ru(NH_3)_6Cl_3$ in 0.1 M lithium acetate–acetic acid buffer (pH 4.5). The

† Arthur Amos Noyes Laboratories.
‡ Laboratoire d'Electrochimie.

(1) (a) Rubinstein, I.; Bard, A. J. *J. Am. Chem. Soc.* **1980**, *102*, 6641. (b) Rubinstein, I.; Bard, A. J. *J. Am. Chem. Soc.* **1981**, *103*, 5007. (c) Henning, T. P.; White, H. S.; Bard, A. J. *J. Am. Chem. Soc.* **1981**, *103*, 3937. (d) White, H. W.; Leddy, J.; Bard, A. J. *J. Am. Chem. Soc.* **1982**, *104*, 4811. (e) Martin, C. R.; Rubinstein, I.; Bard, A. J. *J. Am. Chem. Soc.* **1982**, *104*, 4817. (f) Krishnan, M.; Zhang, X.; Bard, A. J. *J. Am. Chem. Soc.* **1984**, *106*, 7371.

(2) (a) Buttry, D. A.; Anson, F. C. *J. Electroanal. Chem.* **1981**, *130*, 333. (b) Buttry, D. A.; Anson, F. C. *J. Am. Chem. Soc.* **1982**, *104*, 4824. (c) Buttry, D. A.; Anson, F. C. *J. Am. Chem. Soc.* **1983**, *105*, 685. (d) Buttry, D. A.; Anson, F. C. *J. Am. Chem. Soc.* **1984**, *106*, 59. (e) Tsou, Y.-M.; Anson, F. C. *J. Electrochem. Soc.* **1984**, *131*, 595. (f) Buttry, D. A.; Saveant, J.-M.; Anson, F. C. *J. Phys. Chem.* **1984**, *88*, 3086.

(3) (a) Andrieux, C. P.; Dumas-Bouchiat, J. M.; Saveant, J.-M. *J. Electroanal. Chem.* **1978**, *87*, 39. (b) *J. Electroanal. Chem.* **1978**, *87*, 55. (c) *J. Electroanal. Chem.* **1978**, *88*, 43. (d) *J. Electroanal. Chem.* **1980**, *113*, 1. (e) *J. Electroanal. Chem.* **1980**, *113*, 19.

(4) Lee, C.-W.; Gray, H. B.; Maimstrom, B. G.; Anson, F. C. *J. Electroanal. Chem.* **1984**, *172*, 289.

(5) Pladziewicz, J. R.; Meyer, T. J.; Broomhead, J. A.; Taube, H. *Inorg. Chem.* **1973**, *12*, 639.

0002-7863/85/1507-3442$01.50/0 © 1985 American Chemical Society